

On scaling the mean momentum balance and its solutions in turbulent Couette–Poiseuille flow

By TIE WEI¹, PAUL FIFE² AND JOSEPH KLEWICKI³

¹Department of Mechanical and Nuclear Engineering, Penn State University,
State College, PA 16802, USA

²Department of Mathematics, University of Utah, Salt Lake City, UT 84112, USA

³Department of Mechanical Engineering, University of New Hampshire, Durham, NH 03824, USA

(Received 19 August 2005 and in revised form 11 August 2006)

The statistical properties of fully developed planar turbulent Couette–Poiseuille flow result from the simultaneous imposition of a mean wall shear force together with a mean pressure force. Despite the fact that pure Poiseuille flow and pure Couette flow are the two extremes of Couette–Poiseuille flow, the statistical properties of the latter have proved resistant to scaling approaches that coherently extend traditional wall flow theory. For this reason, Couette–Poiseuille flow constitutes an interesting test case by which to explore the efficacy of alternative theoretical approaches, along with their physical/mathematical ramifications. Within this context, the present effort extends the recently developed scaling framework of Wei *et al.* (2005*a*) and associated multiscale ideas of Fife *et al.* (2005*a, b*) to fully developed planar turbulent Couette–Poiseuille flow. Like Poiseuille flow, and contrary to the structure hypothesized by the traditional inner/outer/overlap-based framework, with increasing distance from the wall, the present flow is shown in some cases to undergo a *balance breaking* and *balance exchange* process as the mean dynamics transition from a layer characterized by a balance between the Reynolds stress gradient and viscous stress gradient, to a layer characterized by a balance between the Reynolds stress gradient (more precisely, the sum of Reynolds and viscous stress gradients) and mean pressure gradient. Multiscale analyses of the mean momentum equation are used to predict (in order of magnitude) the wall-normal positions of the maxima of the Reynolds shear stress, as well as to provide an explicit mesoscaling for the profiles near those positions. The analysis reveals a close relationship between the mean flow structure of Couette–Poiseuille flow and two internal scale hierarchies admitted by the mean flow equations. The averaged profiles of interest have, at essentially each point in the channel, a characteristic length that increases as a well-defined ‘outer region’ is approached from either the bottom or the top of the channel. The continuous deformation of this scaling structure as the relevant parameter varies from the Poiseuille case to the Couette case is studied and clarified.

1. Introduction

Purely shear-driven flow in a plane channel becomes turbulent when the applied steady wall motion is sufficiently large. Similarly, purely pressure-driven flow in the same duct will become turbulent when the applied pressure gradient is large enough. Broadly speaking, a primary requirement in either case is that the applied driving mechanism impart momentum sufficient to sustain the mechanisms of wall-bounded

turbulence. The process by which momentum is applied, however, differs between these two flows. In Couette flow, the momentum is input locally (i.e. at the wall), and the internal dynamics subsequently act to transmit it throughout the flow. Conversely, in Poiseuille flow momentum is imparted through the action of a uniform mean differential pressure force. In either case, however, the driving mechanisms, in conjunction with no-slip walls and the intrinsic turbulent dynamics, serve to create large near-wall curvature in the mean velocity profile in concert with large gradients of the Reynolds stress. These constitute common attributes that are central to the generation and maintenance of turbulence in both of these flows. A broad objective of the analysis provided herein is to further elucidate the connections between the driving mechanisms of these flows and the scaling behaviours of their statistical structure.

Consideration of the differences and commonalities between Couette and Poiseuille flow naturally leads to enquiries regarding the scaling behaviours and mathematical structure in the combined Couette–Poiseuille (C-P) scenario. There have been a number of efforts along these lines, including El Telbany & Reynolds (1980), Schlichting & Gersten (2000), Nakabayashi *et al.* (2004). Most notable among these are treatments using traditional concepts of inner- and outer-scaling regions, often along with inner/outer overlap ideas having their beginnings in the work of Izakson (1937) and Millikan (1939). Any theoretical study of these turbulence issues based on exact models such as the Navier–Stokes equations will necessarily be incomplete because of analytical difficulties with those models. Therefore, among such incomplete studies, it is important, if possible, to examine a variety of alternative approaches. Insight is promoted by diverse viewpoints.

The viewpoint in this paper is that understanding the local scaling structure of the mean velocity and Reynolds stress profiles is a primary objective. In fact it leads to much further information about those profiles, as well as a few conceptual differences from previous papers by other authors.

For example, in the case of Couette flow the outer scale is shown (as in Fife *et al.* 2005*b*) to arise as the culminating scale of a hierarchy that is a direct consequence of the dynamical balance everywhere between the viscous and Reynolds stress gradients. Physically, this origin for the outer length in Couette flow is distinctly different from the classical notion that it is associated with a *turbulent core region* within which the dynamical effects of viscosity are small compared with turbulent inertia. On the other hand, in Poiseuille flow there is the empirical fact that the extent of the traditionally defined logarithmic law region covers three subdomains whose underlying mean dynamics are distinct (Wei *et al.* 2005*a*) – adding complexity to the notion that this layer (as traditionally defined) constitutes an inertial sublayer in physical space (e.g. Tennekes & Lumley 1972).

Relevant, however, to the theoretical framework employed herein, some previous approaches/observations are particularly noteworthy. These relate to the combined use of shear stress information from both walls to scale data, and, more generally, the importance of the stress gradients in describing dynamical structure (El Telbany & Reynolds 1980, 1981; Thurlow & Klewicki 2000; Nakabayashi *et al.* 2004).

The present effort aims to provide firm evidence that a unified theoretical framework for C-P flow not only exists, but is a rational extension of a theoretical framework that successfully describes the scaling behaviours of Couette and Poiseuille flows individually; see Wei *et al.* (2005*a*), Fife *et al.* (2005*a,b*), Klewicki *et al.* (2004); Wei *et al.* (2005*b*). A significant feature of the present treatment is that it is entirely independent of the traditional inner/outer/overlap framework.

The mathematical framework is outlined in §§2, 3, and 4, with an explanation of the mesolayer analysis, along with its implications on the properties of the mean velocity and Reynolds stress profiles, given in §5. Section 6 deals with continua of ‘scaling patches’, as introduced in Fife *et al.* (2005*a,b*). A scaling patch is defined to be a region in the flow field specified by an interval of distances from the wall, together with a scaling or non-dimensionalization of the variables which is natural for that region. Here natural means, on the one hand, that data utilizing a variety of different values of the appropriate Reynolds number appear independent of Reynolds number when plotted in the form of normalized variables. (The traditional inner and outer normalizations satisfy this criterion near the wall and near the centreline.) Secondly, the resulting plots should not collapse to constants anywhere in the region being considered; i.e. the scaled dependent variables (or at least one of them) should depend nontrivially on the scaled distance from the wall. If this dependence collapses to a constant, the scaled distance under consideration is too large and is not the natural distance scaling for that part of the patch. In this case either the scaling in the patch should be changed or the patch region should be reduced. For example, if the inner scaling is used in the meso-region, as is often advocated, it leads to the wrong characteristic length there. Consequently, it does not produce a scaling patch, and does not in itself convey detailed information about the scaling structure of the profiles that scaling patches provide. In previous publications, scaling patches have sometimes been called ‘layers’, but in the present paper that term is reserved for a different related concept, the ‘physical layers’ introduced in §2. The analysis given here applies only when statistically stationary turbulence occupies the entire channel.

To reiterate, under the conviction that knowledge of the local scaling properties of the mean momentum and Reynolds stress profiles are basic to understanding wall-bounded turbulent flow, this paper seeks to obtain this knowledge in the case of Couette–Poiseuille flow by finding all possible scaling patches. The procedure is to use assumed criteria to identify such patches at specific locations.

Using this procedure, it is shown in §6 that continua (pairs of such continua, generally) of scaling patches exist for C-P flow, as they do for pure Couette and Poiseuille flows, and that certain pivotal locations in the channel are identified as the loci of outer regions, where the characteristic lengths for the solution profiles are maximal.

The qualitative nature of the transition, via C-P flow and parameter variation, from Couette to Poiseuille flow is also taken up in §7, and a discussion/review follows in §8.

2. Mean momentum balance framework for Couette and Poiseuille flows, and its extension to C-P flows

This section reviews the application of the mean momentum balance-based framework to planar Poiseuille and Couette flow, and proposes its extension to combined C-P flow. Only a brief outline of the essential features are presented here; the reader is referred to the studies of Wei *et al.* (2005*a*) and Fife *et al.* (2005*a,b*) for a more detailed analysis of the pure Poiseuille and Couette flows, as well as of the rigorous transformation that connects them. The same theoretical framework is employed in both of the ‘pure’ cases, and it will be shown to be applicable to the combined C-P flow as well.

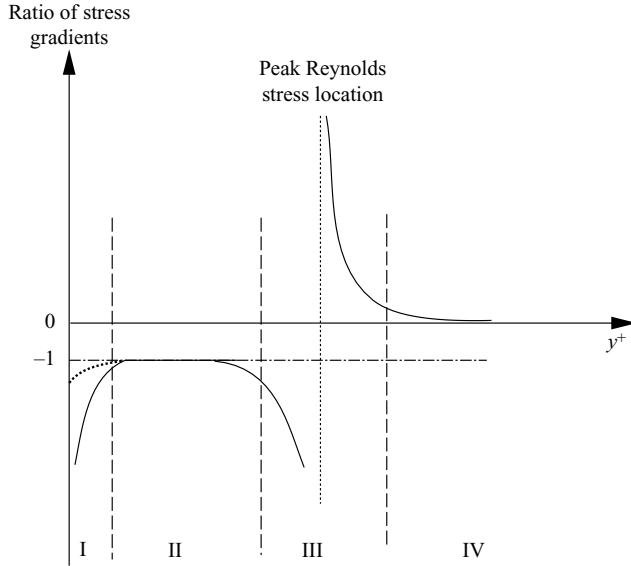


FIGURE 1. Sketch of the physical layer structure of turbulent Poiseuille and Couette flow. For Poiseuille flow layer I is the inner viscous stress gradient/pressure gradient balance layer. Layer II is the viscous stress/Reynolds stress gradient balance layer. Layer III is the mesolayer in which all terms are important, and in layer IV the Reynolds stress gradient and pressure gradient balance. For Couette flow the entire flow is characterized by an exact balance between the Reynolds stress and viscous stress gradients, so that only layer II appears.

2.1. Force balance structure

For fully developed axial flow between infinite parallel plates spaced a distance 2δ apart (figure 2), the x -component of the Reynolds-averaged Navier–Stokes equation reduces to

$$0 = -\frac{1}{\rho} \frac{dP}{dx} + \nu \frac{d^2 U}{dy^2} + \frac{dT}{dy}, \quad (2.1)$$

where U is the mean axial velocity, P is the mean pressure (its x -derivative is constant) and $T = -\langle uv \rangle$ is the Reynolds shear stress, u and v being the components of the velocity fluctuation. Equation (2.1) applies equally to the Poiseuille, Couette, and C-P flow, although in Couette flow the pressure gradient term is identically zero.

Under the present framework, the dynamically relevant principal layer structure for the flow is revealed by considering the relative magnitudes of the terms in the mean momentum balance. This may be accomplished by examining the ratio of the second and third terms in (2.1). In this way, figure 1 shows the layer structure for these flows in the pure Couette and Poiseuille cases (since there is symmetry with respect to the centreline, figure 1 covers only half of the channel). As discussed by Wei *et al.* (2005a), to leading order the mean dynamical structure of Poiseuille flow consists of a pressure gradient/viscous stress gradient balance layer (I), a Reynolds stress gradient/viscous stress gradient balance layer (II), a mesolayer in which all three terms are of nominally the same order of magnitude (III), and an outer layer in which the pressure and Reynolds stress gradients balance (IV). For Couette flow the mean dynamical structure is much simpler, consisting entirely of layer II, so that the ratio expressed in figure 1 is -1 everywhere.

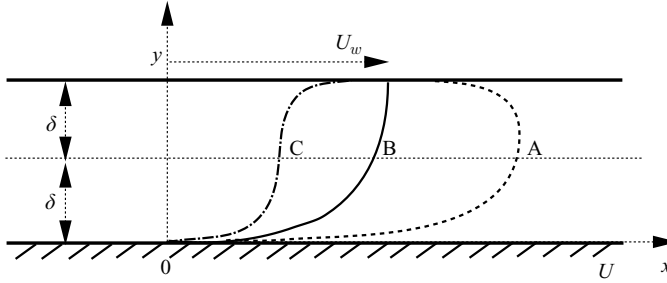


FIGURE 2. Schematic depictions of the mean velocity distributions in C-P flow for fixed upper wall velocity U_w and different degrees of asymmetry. Profile A is a typical Poiseuille-type flow. Profile B represents an intermediate type, and Profile C is a typical Couette-type flow.

For either a pure *Poiseuille* flow or a combined C-P flow, a global force balance between the pressure gradient and the wall friction, which is a necessary condition for existence of a steady flow, can be found (e.g. Panton 1984) by integrating (2.1) over the channel:

$$-2 \frac{\delta}{\rho} \frac{dP}{dx} + \left[\nu \frac{dU}{dy} \right]_{y=0}^{y=2\delta} = 0; \quad (2.2)$$

here the brackets denote the difference between the upper and lower values.

With no loss of generality, it will always be assumed that:

- (a) the shear stress at the upper wall, in magnitude, is no greater than that at the lower wall, and
- (b) the lower wall shear stress is positive.

Thus

$$\left| \frac{dU}{dy} \right|_{y=2\delta} \leq \left. \frac{dU}{dy} \right|_{y=0}. \quad (2.3)$$

If, in fact, (a) is violated, then one simply interchanges the upper and lower walls to obtain an equivalent problem in which (a) holds. Similarly if (b) is violated, one reverses the signs of all velocities. To put (a) in other words, the convention will be always to position the origin of the y coordinate at the wall with the higher magnitude of shear stress.

Sketches of possible C-P mean profile types are shown in figure 2. As indicated, the possibilities are divided roughly into three types: Poiseuille-type flow, intermediate flow and Couette-type flow, indicated by curves A, B and C, respectively. They correspond to the cases when the upper wall shear stress is (relative to the lower one) positive and significant, small, and negative and significant. An elaboration of this classification, as well as a study of the features of the transition between Couette and Poiseuille flows as a parameter is varied, will be given in §7.

2.2. Generic elements of the multiscale analysis

One primary component of the multiscale analysis is to seek normalized forms of the equation of motion that reflect the appropriate dominance of terms as revealed through an examination of momentum balance data. The notion of dominance will be under the condition that a basic singular perturbation parameter ϵ be small: $\epsilon \ll 1$. It is defined by $\epsilon^2 \sim 1/Re_\tau$, where Re_τ is a wall Reynolds number based on the lower wall. There is also such a Reynolds number based on the upper wall, but the arrangement of the walls will always be taken so that the number attached to the

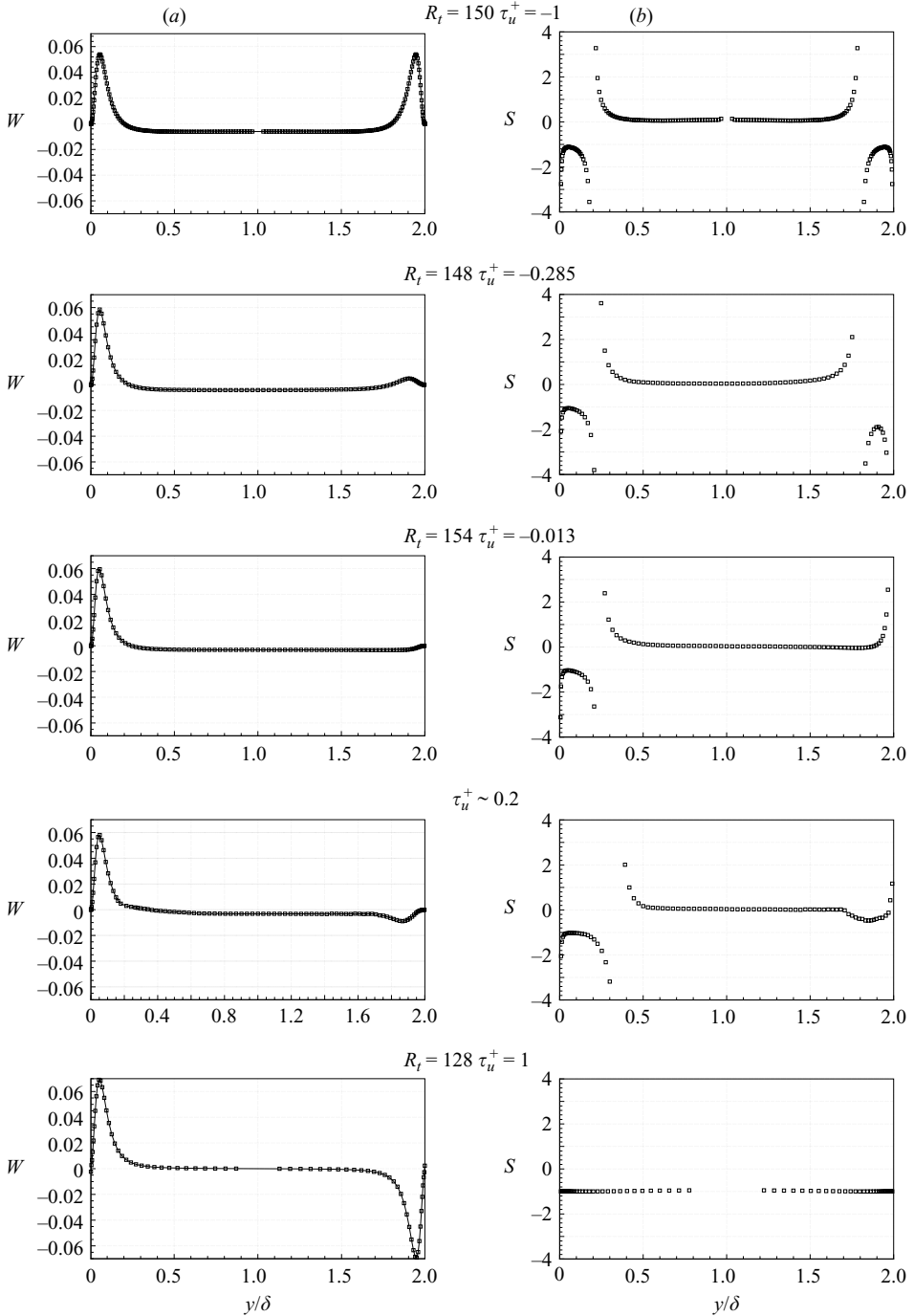


FIGURE 3. (a) $W = dT^+/dy^+$; (b) ratios S of the viscous stress gradient to Reynolds stress gradient in C-P flow for various values of τ_u^+ , a parameter on the continuum between Couette ($\tau_u^+ = 1$) and Poiseuille ($\tau_u^+ = -1$) flow. A transition from Poiseuille to Couette is represented by the passage from top to bottom. Note that while the range of wall motions represented is relatively small, the limiting cases of pure Poiseuille and Couette flow described relative to figure 1 have been previously confirmed by Wei *et al.* (2005a) and Fife *et al.* (2005b) respectively. Note that the same ratio S is plotted in figures 1 and 3, but in figure 1, only half of the channel is covered, the whole channel being shown in the present figure.

lower wall is the larger of the two; all the analysis will be with respect to the larger Reynolds number.

The inner-normalization, producing U^+ and T^+ for example, will utilize the friction velocity at the lower wall. The goal then is to determine the normalization such that the *nominal* orders of magnitude of the terms as $\epsilon \rightarrow 0$ matches their *actual* orders of magnitude in some subdomain. In this way the proper equation for each subdomain (scaling patch; Fife *et al.* 2005a) is, to leading order, parameter-free. This procedure generally succeeds for all the scaling patches that have been found. For Poiseuille flow it requires a rescaling for layer III, for example, that generates a parameter-free normalized form of (2.1) while retaining all three terms (Wei *et al.* 2005a). The inner-scaling, for which the law of the wall holds, is valid in layer I and part of layer II; see a more complete discussion of scaling in these layers in the Appendix.

An analogous phenomenon in fact occurs for a whole continuum of scalings, as shown in Fife *et al.* (2005a, b). In the case of layer III, from this rescaling a new fundamental length scale (the mesoscale) is identified (having the same theoretical justification as the traditional inner and outer scales). The scaling patches, including the mesolayer, were revealed in Wei *et al.* (2005a) to be connected through a *balance breaking* and *balance exchange* of terms.

In addition to ϵ , there is only one other parameter that determines the flow characteristics. It is the ratio τ_u^+ (3.8) of the friction forces, per unit length, exerted on the upper and lower walls by the flow. It is limited to the range $|\tau_u^+| \leq 1$, and measures the relative magnitude of the Poiseuille vs Couette effect. It does not introduce any singular perturbation complications.

Analysis of Couette flow by Fife *et al.* (2005b) reveals that, generally, within any stress gradient balance layer the mean equation of motion admits a hierarchy (continuum) of scaling patches. The transformation (adjusted Reynolds stress function) employed to accomplish this is an extension of that which renders the governing equation for Couette flow to be identical to that for Poiseuille flow (Fife *et al.* 2005a, b). This identity allows the hierarchy results, originally obtained for Couette flow, to be transferred to Poiseuille flow as well.

As intuitively anticipated, it is shown herein that a similar layer hierarchy underlies the structure of C-P flow. Overall, the present approach places C-P flow in a context that can be rationally connected to the mathematical and physical structures of Couette and Poiseuille flow. Thus, among many other things, the self-consistent scaling behaviour of the Reynolds shear stress and mean velocity are made apparent (§ 5.3).

2.3. Principal layers for the combined Couette–Poiseuille problem

As for the pure Poiseuille case, the mean momentum equation for Couette–Poiseuille flow is given by (2.1). As before, it is useful to examine the stress gradient ratios. Let

$S =$ ratio of the viscous stress gradient to the Reynolds stress gradient.

Figure 3(a) shows S for a range of five C-P flow conditions. (The graphs located second from the bottom in that figure are not based on actual data, which are unavailable; rather they are qualitative depictions of surmised trends.) The principal

The pure Poiseuille flow data ($\tau_u^+ = -1$) are from the DNS of Iwamoto, Suzuki & Kasagi (2002). The Couette–Poiseuille flow data ($\tau_u^+ = -0.285, -0.013$) are from the DNS of Kuroda, Kasagi & Hirata (1994). The pure Couette flow data ($\tau_u^+ = 1$) are from DNS of Shingai, Kawamura & Matsuo (2000). Since no DNS data are available for the Couette-type flow shown second from the bottom, a heuristic sketch is provided showing the expected trend (see also § 7.3).

layers are characterized by S being approximately -1 , 0 , or being unbounded, so that two of the three forces are dominant. It will be shown that the physical layer structure, as well as the scaling structure, of C-P flow are closely related to the function W on figure 3(b). That function is the inner-scaled Reynolds stress gradient. This aspect will be explored in some depth in §6 as well as §7. In particular, pure Couette flow contains one internal zero in d^2U^+/dy^{+2} , together with one peak and one valley in $dT^+/dy^+ \equiv W$, while pure Poiseuille flow contains one minimum in d^2U^+/dy^{+2} and two peaks in W . Thus, in the transition from a Couette-dominated to a Poiseuille-dominated flow, a valley in the Reynolds stress gradient W changes into a second peak.

The peculiar features of the graph of S in the case second from the bottom of that figure are discussed in §7.3.

Before ascribing physical or mathematical significance to the behaviours reflected in figure 3, it is useful to identify a particularly pertinent and nonintuitive trend associated with variations in τ_u^+ (the aforesaid ratio of tangential wall forces). Specifically as τ_u^+ varies from -1 (pure Poiseuille flow) toward $\tau_u^+ = 1$ (pure Couette flow), the inertially dominated region where $S \approx 0$ initially grows until it encompasses almost the entire upper half of the channel. It is known, however, that that entire mean flow must eventually resemble its limiting stress gradient balance layer structure. Thus, with further increases in the Couette component (not shown) the inertial region must eventually diminish. A description of the route by which this occurs is a primary objective of this paper (see especially §7.3).

As was noted, for any given parameter values, C-P flow is established through the combination of the two distinctly different driving mechanisms. In the pure Couette limit, that mechanism acting alone promotes the establishment of a layer II (stress gradient balance layer) structure across virtually the entire flow, while the Poiseuille mechanism seeks to establish the four-layer structure depicted in figure 1. Thus, as a pressure gradient is increasingly imposed on the pure Couette condition, it is rational to anticipate the eventual emergence of a centrally positioned inertial subdomain (IV). As indicated in figure 3, however, the transitions between the limiting states are not attained by such intuitively obvious routes.

It is shown in §7.2 that the core region in the various right-hand parts of figure 3, where (except for the bottom one) the ratio S is near 0, should be considered the amalgam of two core regions, associated with two different hierarchies, on the left and right.

3. The inner-normalized momentum balance equation

The derivation of the inner formulation of (2.1) is now described.

3.1. Choosing the parameters

In either pure Poiseuille or Couette flow, global Reynolds numbers could be defined using the centreline velocity (or wall velocity for Couette flow) or bulk mean velocity. In scaling analyses of either of these flows, however, the Reynolds number is almost exclusively defined using the friction velocity; i.e. in the case of pure Couette or pure Poiseuille flow, $Re_\tau = u_\tau \delta / \nu$, with u_τ given by (3.1). Relative to the driving mechanisms discussed in §1, this would seem to have the strongest physical justification. That is, in Couette flow the wall motion imposes a shear at the wall, while in Poiseuille flow the wall shear stress is directly proportional to the applied mean pressure gradient. Under C-P flow also it is rational to anticipate that these physical influences should

still be reflected via the wall shear stress behaviours. (It is relevant to note that El Telbany & Reynolds (1981) suggested an effective friction velocity that combines the shear stress information from the two walls, i.e. $u_e = (u_{\tau 1} + u_{\tau 2})/2$.)

Given these considerations, the choice of Reynolds number in this paper is not based on, say, the bulk mean velocity (e.g. El Telbany & Reynolds 1980), but rather on the greater of the two friction velocities. The other relevant parameter τ_u^+ (see (3.8)) can be thought of as measuring the degree to which the profile symmetries inherent to either Couette or Poiseuille flow are disrupted. In dimensionless form, the solution of the mean momentum equation depends on these two parameters Re_τ , τ_u^+ alone.

3.2. The inner equations

The friction velocity is therefore defined by

$$u_\tau^2 = \nu \left. \frac{dU}{dy} \right|_{y=0}, \quad (3.1)$$

and is used to scale all velocities: $U = u_\tau U^+$, $T = u_\tau^2 T^+$. The inner-normalized wall-normal coordinate is

$$y^+ = \frac{u_\tau}{\nu} y. \quad (3.2)$$

Non-dimensionalizing (2.1) and (2.2) in this way provides

$$-\frac{1}{\rho} \frac{dP}{dx} \frac{\nu}{u_\tau^3} + \frac{d^2 U^+}{dy^{+2}} + \frac{dT^+}{dy^+} = 0 \quad (3.3)$$

and

$$-2 \frac{\delta}{u_\tau^2} \frac{1}{\rho} \frac{dP}{dx} + \left[\frac{dU^+}{dy^+} \right]_{y=0}^{y=2\delta} = 0, \quad (3.4)$$

respectively.

The inner Reynolds number is defined by $Re_\tau = \delta u_\tau / \nu = \delta^+$, and a small parameter by

$$\epsilon^2 = Re_\tau^{-1}. \quad (3.5)$$

Using these symbols and eliminating dP/dx from (3.3) and (3.4), one obtains

$$-\frac{1}{2} \epsilon^2 \left[\frac{dU^+}{dy^+} \right]_{y=0}^{y=2\delta} + \frac{d^2 U^+}{dy^{+2}} + \frac{dT^+}{dy^+} = 0. \quad (3.6)$$

Note that in all cases, the normalization has been chosen so that

$$\frac{dU^+}{dy^+}(0) = 1. \quad (3.7)$$

In the *Poiseuille case*, the shear stress at the upper wall is equal in magnitude but of opposite sign as that at $y^+ = 0$, so that from (3.7),

$$\left[\frac{dU^+}{dy^+} \right]_{y=0}^{y=2\delta} = -2,$$

and (3.6) becomes

$$\epsilon^2 + \frac{d^2 U^+}{dy^{+2}} + \frac{dT^+}{dy^+} = 0.$$

In the *Couette case*, the shear stress at the upper wall is the same as that at the lower wall, so that

$$\left[\frac{dU^+}{dy^+} \right]_{y=0}^{y=2\delta} = 0,$$

and (3.6) becomes

$$\frac{d^2U^+}{dy^{+2}} + \frac{dT^+}{dy^+} = 0.$$

The function U^+ is odd with reference to the centreline, while the profile of T^+ is an even function. The opposite is true in Poiseuille flow; none of these symmetries exist in C-P flow.

The general case. When both Couette and Poiseuille effects are present, it will be convenient to use the following symbol for the inner-normalized friction at the upper wall:

$$\tau_u^+ = \left. \frac{dU^+}{dy^+} \right|_{y^+=2\delta^+}, \quad (3.8)$$

i.e. the ratio of shear forces at the two walls (it could be positive or negative). The new momentum balance equation is

$$\frac{1}{2}\epsilon^2(1 - \tau_u^+) + \frac{d^2U^+}{dy^{+2}} + \frac{dT^+}{dy^+} = 0. \quad (3.9)$$

There are boundary conditions to be appended to (3.9):

$$U^+(0) = 0, \quad \frac{dU^+}{dy^+}(0) = 1, \quad T^+(0) = 0, \quad (3.10)$$

and

$$\frac{dU^+}{dy^+}(2/\epsilon^2) = \tau_u^+, \quad T^+(2/\epsilon^2) = 0, \quad (3.11)$$

where it is noted that the upper wall location is at $y^+ = 2\delta^+ = 2\epsilon^{-2}$.

It is seen that ϵ and τ_u^+ are the only two independent parameters appearing in (3.9), (3.10), and (3.11). It will be assumed that $0 < \epsilon \ll 1$. The allowed range of τ_u^+ , according to (2.3), is

$$|\tau_u^+| \leq 1. \quad (3.12)$$

The pure Couette and Poiseuille cases are recovered when τ_u^+ is at one of the two ends of the allowed interval. All values in-between are possible, and each provides (for a given small ϵ) its own U^+ and T^+ profile.

There turns out to be a wealth of scaling patches for the solution U^+ , T^+ , due to the smallness of ϵ . This aspect of the mean profiles will be examined in §6. The other parameter τ_u^+ is not of a singular perturbation type; its physical role is as a measure of the relative magnitudes of the effect of the differential wall velocities, versus the pressure gradient effect. Its mathematical role is mainly to determine how the multiplicity of scaling patches are distributed across the channel.

4. Outer-normalized equations

The outer-normalized distance is defined by

$$\eta = \epsilon^2 y^+. \quad (4.1)$$

Under the present definitions, the mean momentum equation for C-P flow takes the

outer-normalized form,

$$0 = \frac{1}{2}(1 - \tau_u^+) + \epsilon^2 \frac{d^2 U^+}{d\eta^2} + \frac{dT^+}{d\eta}. \quad (4.2)$$

Note that in the pure Poiseuille case, the first term on the right of (4.2) equals 1, under intermediate flow as defined before it equals $\frac{1}{2}$, and for pure Couette flow it equals 0. Furthermore, examination of the stress gradient ratios S in figure 1 reveals that in layer IV in the Poiseuille case, the second term is small, and thus the mean momentum equation is satisfied by a balance between the pressure gradient and Reynolds stress gradient. In C-P flow, however, when the Couette component is large the first term in (4.2) will become small, and thus under such conditions the second term cannot be neglected. Therefore, as pure Couette flow is approached (from the Couette flow side of the intermediate profile), layer IV diminishes in extent and is replaced by layer II. In this limit the entire mean momentum field is characterized by a balance between the viscous and Reynolds stress gradients.

5. Couette–Poiseuille mesolayer structure

Beyond the traditional inner- and outer-scalings, the general features of the present scaling theory were briefly discussed in §2.2. Distinctive among these is the mathematical description by which the inner and outer physical layers are connected. Specifically, for flows with an increasingly significant Poiseuille component, the present mathematical framework predicts the existence of an outer physical layer (IV) whose dynamics are increasingly well-approximated by a balance between the Reynolds stress gradient and the applied mean pressure gradient.† Under this condition, a third physical layer within the flow emerges (the mesolayer, layer III), and it coincides with a characteristic scaling patch. Across this layer the inner and outer layers are then connected through the *balance breaking* and *balance exchange* process described by Wei *et al.* (2005a).

It has been known for a long time (possibly beginning with Afzal 1982; see other citations in Wei *et al.* 2005a, as well as Antonia *et al.* 1992 and Sreenivasan 1989) that a special scaling for turbulent Poiseuille flow is appropriate in a region (it turns out to be a scaling patch) encompassing where the Reynolds stress attains its maximum. That region coincides with the mesolayer, and its length-scaling factor is the geometric mean of those yielding the inner and outer length scalings. The existence of such a region, and its identification as a scaling patch, was verified by means of a balance exchange argument in Wei *et al.* (2005a) and Fife *et al.* (2005b).

In the case of turbulent Couette flow, there is still a scaling patch located where the Reynolds stress has its maximum, but this time that maximum is at the centreline (Fife *et al.* 2005a, b). The length scale in that patch coincides with the traditional outer length scale (4.1), but the scaled form of the momentum balance in that patch is not the traditional outer approximation. Rather, it is

$$\frac{d^2 U^+}{d\eta^2} + \frac{d\hat{T}}{d\eta} = 0,$$

where \hat{T} is the mesoscaled Reynolds stress given by (5.1) below. This preserves its

† Regarding this, note that for pure Couette flow the present theory asserts that there is no such outer physical layer (e.g. Fife *et al.* 2005b), whereas the traditional theory asserts that an outer layer, within which viscous effects are negligible, exists even for pure Couette flow (e.g. Libby 1996). An outer-scaling region, however, does exist.

meaning as a balance between viscous and turbulent forces. The patch also constitutes the culminating scaling associated with the largest of a hierarchy of patches composing the structure of the stress gradient balance layer.

In what follows, an analysis pertaining to the mesolayer in C-P flow is presented. It will be assumed that the flow has an important Poiseuille component, in the sense that $1 - \tau_u^+ = O(1)$. The efficacy of this analysis is then tested against its capacity to scale the Reynolds stress profiles over a range of C-P flow conditions.

5.1. The mesoscale

The inner and outer subdomains have y^+ and η as characteristic distance variables. The physical mesolayer, lying somewhere between the inner and outer domains, is characterized as the place where all of the terms in the momentum balance have the same nominal order of magnitude. In the graphs on the right side of figure 3, the mesolayer corresponds to the region in part (a) of the graph (near the lower wall) where the plotted ratio S transitions from near -1 through $\pm\infty$ to near 0. In the cases considered here, there will generally be a second mesolayer near the upper wall (in figure 3b) as well, where the reverse transition is made.

To reiterate, the mesolayer is defined here physically in terms of the specification of which forces balance in that region. As it turns out, and we shall show, the mesolayer also has a natural scaling, and therefore forms a scaling patch. The origin of the mesoscaling patch is through a balance exchange mechanism described, e.g., in Wei *et al.* (2005a). This patch, as shown in §6, is only one of many such patches forming a collection connecting the inner to the outer scales.

For now, the mathematical strategy is to seek a rescaling of (3.9) that appropriately reflects this description of the mesolayer. This will be possible near the location (call it y_m^+) where T^+ attains its maximum.

The rescaling will take the form

$$y^+ = y_m^+ + \alpha d\hat{y}; \quad T^+ = T_m^+ + \gamma \hat{T}(\hat{y}); \quad (5.1)$$

$$U^+ = U_m^+ + m(y^+ - y_m^+) + \lambda \hat{U}(\hat{y}), \quad (5.2)$$

where α , λ , and γ are scaling parameters, functions of ϵ to be determined, and $m = (dU^+/dy^+)(y^+ = y_m^+)$, unknown at this point. All quantities with hats, together with their derivatives, are $O(1)$ inside the prospective scaling patch, defined say as $\{|\hat{y}| \leq O(1)\}$; and the quantities with subscript m are the values of those variables at the maximum point y_m^+ of T^+ . The parameter α can be thought of as a characteristic length in that patch, λ is a characteristic increment in U^+ , and similarly for γ .

Theory would tell us that λ can be arbitrarily chosen, as long as γ and α are chosen appropriately in terms of λ . Relevant to this, experimental evidence shown in Wei *et al.* (2005a) reveals that the normalized velocity increment across layer III, hence across the mesoscaling patch, is almost identically equal to 1, independent of Reynolds number. Therefore λ will be set equal to 1 in the following. The implications of other possible values of λ are best brought out in the context of the hierarchy of scales in §6, where the same ambiguity reappears. Further discussion on this issue is deferred to that section, as is the discussion of the value of m .

Note that

$$\hat{U}(0) = 0, \quad (5.3)$$

and since T^+ has a maximum at $y^+ = y_m^+$, the analogous relation holds for \hat{T} :

$$\hat{T}(0) = \frac{d\hat{T}}{d\hat{y}}(0) = 0. \quad (5.4)$$

With $\lambda=1$, we pass now to the identification of α and γ . In the patch, by the balance exchange argument elucidated in Wei *et al.* (2005a), all three terms of the momentum balance equation

$$\frac{1}{2}\epsilon^2(1 - \tau_u^+) + \frac{d^2U^+}{dy^{+2}} + \frac{dT^+}{dy^+} = 0 \quad (5.5)$$

have to have the same order of magnitude. From (5.1) and (5.2),

$$\frac{d^2U^+}{dy^{+2}} = \frac{1}{\alpha^2} \frac{d^2\hat{U}}{d\hat{y}^2}, \quad \frac{dT^+}{dy^+} = \frac{\gamma}{\alpha} \frac{d\hat{T}}{d\hat{y}}. \quad (5.6)$$

As mentioned, a successful rescaling results in the normalized variables and their derivatives, such as $d^2\hat{U}/d\hat{y}^2$ and $d\hat{T}/d\hat{y}$, remaining $\leq O(1)$ over an $O(1)$ variation in the appropriately scaled layer thickness (flow subdomain or scaling patch; Fife *et al.* 2005a), which is being taken here to be $\{|\hat{y}| \leq 1\}$. By the requirement established above, for the mesolayer this demands that the orders of magnitude $1/\alpha^2$ and γ/α must match the third term in (5.5), which will be renamed

$$\epsilon_t^2 \equiv \epsilon^2(1 - \tau_u^+)/2. \quad (5.7)$$

Recall that it is assumed that the Poiseuille component is important. This will be taken to mean that $1 - \tau_u^+ = O(1)$, so that $\epsilon_t = O(\epsilon)$.

Thus one may choose

$$\frac{1}{\alpha^2} = \frac{\gamma}{\alpha} = \epsilon_t^2, \quad (5.8)$$

which requires α and γ to be

$$\alpha = \epsilon_t^{-1} \quad \gamma = \frac{1}{\alpha} = \epsilon_t. \quad (5.9)$$

Furthermore, from (5.1),

$$\hat{y} = \epsilon_t(y^+ - y_m^+) \quad \text{and} \quad \hat{T} = \frac{1}{\epsilon_t}(T^+ - T_m^+). \quad (5.10)$$

Normalization of the mean momentum equation according to these variables results in

$$0 = 1 + \frac{d^2\hat{U}}{d\hat{y}^2} + \frac{d\hat{T}}{d\hat{y}}, \quad (5.11)$$

and thus provides the desired parameter-free representation in which all scaled terms are formally represented as being $O(1)$. Later, the possible existence of a mesolayer near the upper wall will be taken up.

The transformations given by (5.10) inherently characterize mean momentum field behaviours with variations in the composite parameter ϵ_t .

The construction outlined here of the mesoscaling patch relied on the Reynolds stress having a maximum, whose location becomes the seat of the corresponding patch. In §6, the same reasoning will be used to construct a scaling patch at the maximum of each of a family of adjusted Reynolds stresses.

Another analogue is noteworthy. The Reynolds stress attains a minimum at the wall, and there is considerable similarity between the behaviour of the Reynolds stress near that minimal point and its behaviour at the maximum. Despite the similarity, the mesoscale argument cannot be taken over ‘as is’ at the wall to demonstrate the existence of a scaling patch there with different scaling. A patch does exist, but its demonstration requires a major reformulation of the problem. The details of this wall-scaling patch construction and properties are given in the Appendix.

The information in this section will now be employed to describe properties of the Reynolds stress function near its peak.

5.2. Peak Reynolds shear stress location and value

Several papers in the past have addressed the issue of determining the location y_m^+ of the peak Reynolds stress in pure Poiseuille turbulent flow, as well as the maximum value T_m^+ of the Reynolds shear stress. Theoretical approaches to determining the orders of magnitude of these quantities in terms of ϵ have been given; the ones closest in spirit to the present methods were in Wei *et al.* (2005a, 3.21) and Wei *et al.* (2005b). Other references to previous work were given in those papers; note also Antonia *et al.* (1992) and Panton (1997). In most cases, assumptions and methods were used which rely on the existence and properties of an overlap layer for the Reynolds stress profile and (in the case of Panton) an assumed typical explicit form for that profile in the inner region.

Those previous analyses generally can be applied directly to the present analogous situation for Poiseuille-like flows; there is little need to repeat the details. The results are the estimates

$$y_m^+ = O\left(\frac{1}{\epsilon_t}\right) \quad (5.12)$$

and

$$1 - T_m^+ = O(\epsilon_t). \quad (5.13)$$

As an alternative derivation of (5.12), it is noted below following (6.18) that the characteristic length in a member of the hierarchy of patches, to be brought out in §6 below, is asymptotically proportional to its distance from the wall in inner units. In the case of the mesoscale being considered now, that characteristic length, namely α in (5.9), is ϵ_t^{-1} , which should therefore be the location y_m^+ in (5.12). This validates that relation.

5.3. Mesoscaling of the Reynolds shear stress and mean velocity for Poiseuille-like flows

Still assuming that the flow is Poiseuille-like rather than Couette-like, one notes that the form of (5.11) is identical to that using mesoscaling for pure Poiseuille flow. The Reynolds stress and mean velocity should therefore admit the same type of mesoscaling as analytically derived in Wei *et al.* (2005b). To explore this, different scalings of the Reynolds shear stress are shown in figure 4, and the same is done for the mean velocity in figure 5.

Inner-scaling (a) and outer-scaling (b) are, of course, for both T^+ and U^+ the conventional ways of presenting the data. The mesoscaling in figure 4 is from (5.10), and figure 4(c) supports, for the range of Re_τ used, this new scaling for T^+ (but not for U^+) over an interior region of the flow that extends from inside the peak in T^+ to a zone near $y^+ = Re_\tau = \delta^+$. In terms of the mesoscaled variable \hat{y} , this upper limit ranges from 10 to 25 for these data. It should be emphasized that the fact the T^+ can be approximated this way does not mean that the mesoscaling patch itself extends that far; see the discussion of scaling patches in the introduction.

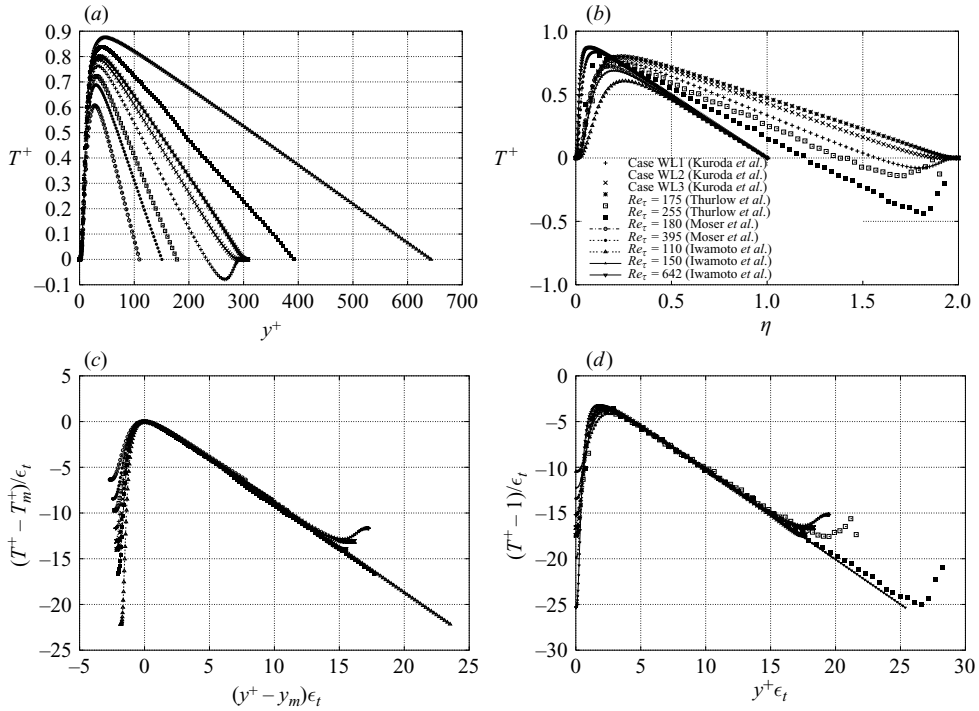


FIGURE 4. Scaling of the Reynolds shear stress in turbulent Couette–Poiseuille flow. (a) Inner-scaling: T^+ vs y^+ . (b) Outer-scaling: T^+ vs η . (c) Mesoscaling: \hat{T} vs \hat{y} . (d) Approximate mesoscaling. The Couette–Poiseuille flow DNS data are from Kuroda *et al.* (1994). They computed three cases of Poiseuille-type flows: WL1: $Re_\tau = 148$, $\tau_u^+ = -0.285$; WL2: $Re_\tau = 152$, $\tau_u^+ = -0.103$; WL3: $Re_\tau = 154$, $\tau_u^+ = -0.013$. The pure Poiseuille flow ($\tau_u^+ = -1$) data are from two sets of DNS by Moser, Kim & Mansour (1999) ($Re_\tau = 180, 395, 590$) and Iwamoto *et al.* (2002) ($Re_\tau = 100, 150, 300, 400, 650$). Two more experimental profiles by Thurlow & Klewicki (2000) are used in (b) and (d). The experimental data are for Couette–Poiseuille flow, $Re_\tau = 175$, $\tau_u^+ = -0.47$ and $Re_\tau = 255$, $\tau_u^+ = -0.68$.

The mesoscaling in figure 5 is from (5.2), and figures 5(c) and 5(d) support this new scaling for U^+ . In this, note has been taken (see the explanation following (6.20)) that the middle term on the right of (5.2) scales the same way as the last term, so that those two terms may be combined into a single term with the properties of the last term.

In this regard, a couple of other points are worth noting.

(a) In narrow regions near the walls, the mesoscaling should not hold, since these are the patches where inner-scalings based upon the local wall shear stress are expected to hold: see Fife *et al.* (2005a). The convincing merging of the profiles in figure 4(a) directly supports this assertion in the vicinity of $y^+ = 0$. More generally, Thurlow and Klewicki (2000) show that local wall shear stress scaling holds in the immediate vicinity of the wall for both positive and negative wall motion. Similarly, the mean velocity data of figure 5(a) convincingly merge to a single curve in the region adjacent to the wall.

(b) As shown for the case of pure Poiseuille flow by previous authors, including Wei *et al.* (2005a), $d\hat{T}/d\hat{y}$ is identically equal to $dT^+/d\eta$. Thus, when referenced to the ‘origin’ value, T_m at y_m , it could be expected that the mesoscaling will provide a good approximation for the Reynolds stress (but clearly not for the mean momentum)

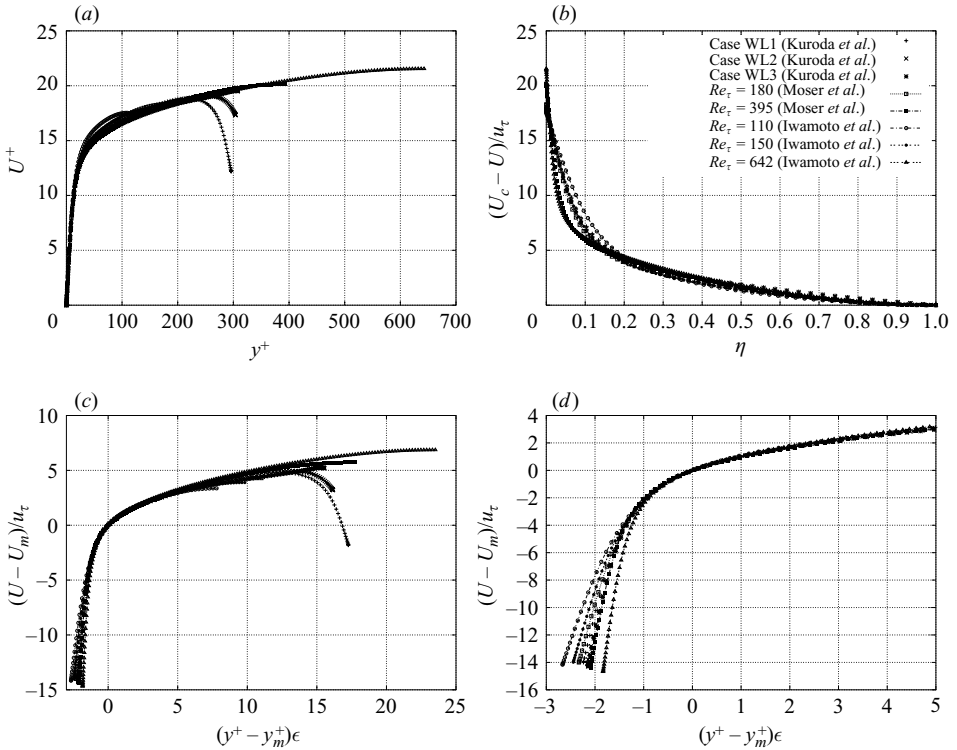


FIGURE 5. Scaling of the mean streamwise velocity in turbulent Couette–Poiseuille flow. (a) Inner-scaling: U^+ vs y^+ . (b) Traditional outer-scaling (velocity defect law): $(U_c - U)/u_\tau$ vs η . (c) Mesoscaling: $(U - U_m)/u_\tau$ vs \hat{y} . (d) Zoom in of the mesoscaling around the mesolayer. The data sources are the same as figure 4.

all the way into any inertial outer layer (layer IV) that might exist. The profiles of figure 4(c) reflect this prediction. In § 6 the existence of a continuum of scaling patches connecting the mesoscaling to the outer-scaling patches will be shown. In the case of the Reynolds stress, the mesoscaling also merges with the scaling in each intermediate patch, resulting in the latter not being recognizable from plots such as those in figure 4. The distinctions among the scalings in the hierarchy are best understood in reference to the scaled variables, including \hat{U} , used in (6.12) and elsewhere in that section, rather than \hat{T} alone.

Lastly, since y_m^+ and T_m^+ are generally not known beforehand, an approximate mesoscaling may be constructed. This scaling is based upon the limiting behaviours of y_m^+ and T_m^+ , and is given by $(T^+ - 1)/\epsilon_\tau$ versus $y^+\epsilon_\tau$. As shown in figure 4(d), this scaling constitutes a very good approximation.

In summary, the derived mesoscaling, applied to both the Reynolds shear stress and mean velocity, serves to merge the various data profiles to a single curve over the range of distances from the wall predicted by the theory.

5.4. Scaling of the Reynolds stress for Couette-like flows

The left-hand plots in figure 3 include some cases of Poiseuille-like and some of Couette-like flows. In all cases, the locations of the maxima of Reynolds stress can be identified as where the function $W = dT^+/dy^+$ changes sign. For each of the Poiseuille-like cases there are two such maxima, one near each of the walls. These

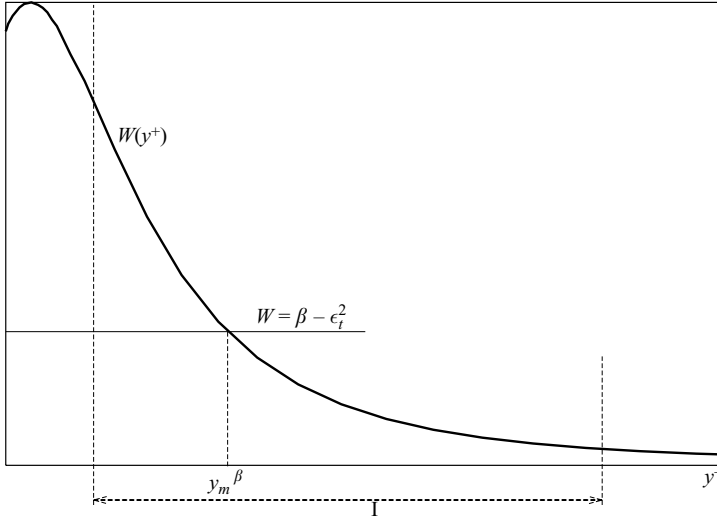


FIGURE 6. Schematic diagram showing the role of the function $W(y^+)$ in determining the relation between β and the location y_m^β of the corresponding scaling patch. The interval I shown here is one of many choices of interval on which W is decreasing.

maxima are also the locations of mesoscaling patches, as described in §5.3. Thus Poiseuille-like flows have two mesoscaling patches, with an outer region somewhere in-between them.

In the Couette-like cases, there is only one change of sign and it is located in the outer region itself. The scaling of the Reynolds stress corresponds to that described in Fife *et al.* (2005b).

6. The hierarchy of scaling patches

Continua of scaling patches, each patch with its own characteristic length, were shown in Fife *et al.* (2005a, b) to exist in pure Couette and pure Poiseuille flows. To extend that argument to the combined case, one looks for basic concepts and features of the flow that are crucial to the existence of such hierarchies. The most important such feature turns out to be the presence of local maxima or minima of the function

$$W(y^+) = \frac{dT^+}{dy^+}(y^+). \quad (6.1)$$

The reasoning will now be explained in the case of a local maximum, leading to a hierarchy covering an interval of y^+ -values adjacent to, and to the right of, the point where the maximum is attained. Later, the argument will be shown to be extendible to the case of a local maximum with hierarchy on the left, or of a local minimum.

6.1. Patch construction

If W has a local maximum at some point $y^+ = y_0^+$, there will be intervals of y^+ -values, located to the right of that point, on which $W(y^+)$ is a decreasing function. Call such an interval I (see figure 6). Rewrite (5.5) in the form

$$W(y^+) = \frac{dT^+}{dy^+} = -\epsilon_t^2 - \frac{d^2U^+}{dy^{+2}}, \quad (6.2)$$

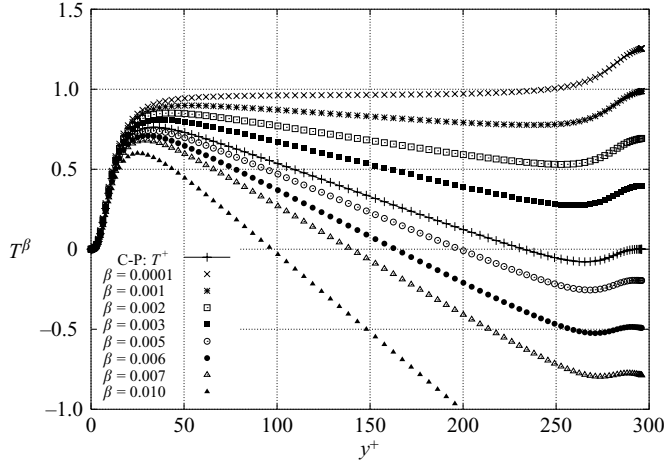


FIGURE 7. The adjusted Reynolds stresses, T^β . The Couette–Poiseuille data are from case WL1 of Kuroda *et al.* (1994), $Re_t = 148$, $\tau_u^+ = -0.285$.

and assume that

$$\frac{d^2 U^+}{dy^{+2}} \leq 0 \text{ on } I. \quad (6.3)$$

Then, according to (6.2),

$$W(y^+) \geq -\epsilon_t^2 \text{ on } I. \quad (6.4)$$

In other words, for each location y^+ inside the interval I , there is a number $\beta \geq 0$ such that

$$W(y^+) = -\epsilon_t^2 + \beta. \quad (6.5)$$

This gives a correspondence between the parameter β and points y^+ in I , as shown in figure 6. To keep things straight, the point corresponding to a given β will be called y_m^β (the reason for this notation will be apparent shortly). It will be shown that a scaling patch exists at each such point y_m^β , and its characteristic length (measured in inner units) is $\beta^{-1/2}$. This is no surprise, because according to (6.2) and (6.5), $(d^2 U^+ / dy^{+2})(y_m^\beta) = -\beta$, and dimensional considerations suggest the stated conclusion.

To proceed, define the artificial ‘adjusted Reynolds stress’ by

$$T^\beta(y^+) = T^+(y^+) + (\epsilon_t^2 - \beta)y^+. \quad (6.6)$$

Examples of adjusted Reynolds stresses are shown in figure 7. Note that each has a maximum when $\beta \geq 0.001$, and the location of that maximum moves toward the wall as β increases. It will be shown that the location is in fact just y_m^β .

From (6.6),

$$\frac{dT^\beta}{dy^+} = W(y^+) + (\epsilon_t^2 - \beta). \quad (6.7)$$

By this and (6.5), the derivative on the left vanishes at $y^+ = y_m^\beta$ and is a decreasing function of y^+ near that point, implying that T^β has a local maximum at $y^+ = y_m^\beta$. This is the meaning of the subscript ‘ m ’. Call the value of T^β at that maximum T_m^β . The correct scaling near y_m^β can again be obtained by a balance exchange argument, which will now be detailed.

By (6.6) and (6.2),

$$\frac{dT^\beta}{dy^+} = -\beta - \frac{d^2U^+}{dy^{+2}}. \quad (6.8)$$

As y^+ approaches y_m^β from below, the term on the left of (6.8) approaches 0, so that there will be a point where its value is the small number β (say); at that point, $d^2U^+/dy^{+2} = -2\beta$ and all three terms in (6.8) have the same order of magnitude. This suggests there should be a rescaling possible such that the three terms are all formally $O(1)$ quantities. That indeed turns out to be the case. We seek scaling factors α , γ , λ , all of them dependent on β , such that the transformation

$$y^+ = y_m^\beta + \alpha \hat{y}, \quad T^\beta = T_m^\beta + \gamma \hat{T}^\beta, \quad U^+ = U_m^+ + m(y^+ - y_m^+) + \lambda \hat{U}, \quad (6.9)$$

where $m = (dU^+/dy^+)(y^+ = y_m^+)$ and \hat{y} , \hat{T} , \hat{U} are $O(1)$ quantities, will produce the desired property of all terms in (6.8) having equal weight. The derivatives occurring in that equation annihilate all linear and constant terms in the expansions for T^β and U^+ in (6.9), so m cannot be determined this way. It will be found by another route, as explained below.

Applying the transformation (6.9) to (6.8) and requiring equal weight produces two equations,

$$\frac{\gamma}{\alpha} = \beta = \frac{\lambda}{\alpha^2}, \quad (6.10)$$

for the three unknowns α , γ , λ . This indeterminacy leads to a family of solutions parametrized by λ . All these parameters depend on β , and there is no contradiction in taking them to be powers of β . Thus the independent parameter λ will be replaced by σ , where $\lambda = \beta^{-\sigma}$ (since we deal with orders of magnitude, there is no need for a constant coefficient in this expression). In all, the family of rescalings are

$$y^+ = y_m^\beta + \beta^{-(\sigma+1)/2} \hat{y}, \quad T^\beta = T_m^\beta + \beta^{-(\sigma+1)/2} \hat{T}^\beta, \quad U^+ = U_m^+ + m(y^+ - y_m^+) + \beta^{-\sigma} \hat{U}, \quad (6.11)$$

This leads to a parameterless equation involving only the scaled quantities \hat{T}^β , \hat{U} , \hat{y} :

$$\frac{d^2\hat{U}}{d\hat{y}^2} + \frac{d\hat{T}^\beta}{d\hat{y}} + 1 = 0. \quad (6.12)$$

It should be emphasized that the rescaling given here will produce new functions with ‘hats’ which may still depend on β , although they have orders of magnitude unity within that particular scaling patch, where $|\hat{y}| \leq O(1)$. This is in accordance with usual practice in asymptotic analysis.

The fact that no parameter appears in (6.12) is evidence that the given β -dependent scalings, producing \hat{y} , \hat{U} , and \hat{T}^β , are candidates for the correct scalings valid near the point y_m^β . But this evidence is independently supported by the fact that the individual terms in (6.12) are known by independent means to equal to -1 , 0 , and 1 , respectively, at the point $\hat{y} = 0$, i.e. $y^+ = y_m^\beta$, which is taken to be the centre of this scaling patch. Similar known values are taken near that point, as shown in the above balance exchange argument. The important observation is that these values of the individual terms are parameter-independent, $\leq O(1)$, and some are $= O(1)$.

There appears to be no theoretical selection mechanism, at this point, to determine the correct value of σ , hence the correct scaling operative in that patch. It will be shown below that the exponent σ , if assumed independent of β (although λ is not, of course), controls the approximate rate of growth of $U^+(y^+)$ in any interval where

the described scaling construction is performed. It will be shown below that the case $\sigma = 0$ corresponds to logarithmic growth, and the other values to power law growth or decay.

It is remarkable that the rescaled momentum balance (6.12) and key values of rescaled quantities are formally independent, not only of β , but also of σ , despite the fact that they reign in different candidate patches, and presumably only one value of σ represents an actual patch.

In previous papers, notably Wei *et al.* (2005a), Fife *et al.* (2005a), and Fife *et al.* (2005b) the above balance exchange construction and rescaling was introduced and pursued. However, in those papers the parameter σ was essentially arbitrarily taken to be 0, and therefore in the latter two cited papers, in which the hierarchy was developed, only logarithmic-like growth was considered.

6.2. The patch at the centreline

The coefficient $\beta^{-(\sigma+1)/2} \equiv \ell(\beta)$ of \hat{y} in (6.11) is the characteristic length (in order of magnitude) of the patch with that value of β . It increases when β decreases, but can grow no larger than the half-width $\delta^+ = \epsilon^{-2}$ of the channel, which is the maximal length scale allowed. That maximal value of ℓ is therefore taken at the value of β such that $\ell(\beta) = \epsilon^{-2}$, i.e. $\beta = \epsilon^{4/(1+\sigma)}$. This length scale will coincide with the traditional length scale η , so that $dy^+ = \epsilon^{-2}d\eta = \epsilon^{-2}d\hat{y}$, where \hat{y} here is the scaled distance in (6.9) for that value of β . The centre y_m^β of the patch, as indicated in (6.9), is a distance $O(1)$ in η from the origin $\{\eta = 0\}$ of the outer coordinate, so up to order of magnitude we may identify $\hat{y} = \eta$ and write functions of \hat{y} as functions of η . It will be shown (see (6.21)) that the right-hand equation in (6.11) can be written

$$U^+ = U_m^+ + \beta^{-\sigma} \tilde{U}(\hat{y}), \quad (6.13)$$

with $\tilde{U}(\hat{y}) = O(1)$.

If $\sigma = 0$, which seems to be the most likely case, this provides the defect law in the outer region. To see this, rewrite (6.13) in terms of the variable η , using the notation $\eta = \eta_m$ as the location where $U^+ = U^+(\eta_m) = U_m^+$. Doing this gives, for some $\eta^* = O(1)$,

$$U^+(1) = U^+(\eta_m) + \tilde{U}(\eta^*), \quad (6.14)$$

and therefore, from (6.13),

$$U^+ = U^+(1) - U^*(1 - \eta) \quad (6.15)$$

for some function $U^*(1 - \eta) = O(1)$ with $U^*(0) = 0$. The traditional defect law is equivalent to (6.15).

Since the use of η as scaled distance in the outer region is now justified, we have the validity of the outer equation (4.2) with the higher-order term neglected: $dT^+/d\eta = -\frac{1}{2}(1 - \tau_u^+)$, with boundary condition $T^+(1) = 0$.

To obtain the dominant expression for U^+ in the core region (still in the case $\sigma = 0$), one would need the function U^* in (6.15). That function is not known; however, the functions U^* (6.15) and $\hat{T}^{\beta=\epsilon^4}$ (6.11) are related through (6.12), which is transformed to

$$\frac{d^2 U^*}{d\eta^2} + \frac{d\hat{T}^{\beta=\epsilon^4}}{d\eta} + 1 = 0. \quad (6.16)$$

Note that this equation satisfies the notion of a scaling patch in that it is both parameter-free and valid over a domain in which $\eta = O(1)$.

An analogous detailed examination of the wall region is given in the appendix.

6.3. Locations of the patches

The analysis will now be continued. To this point, use has merely been made of an interval I of monotonicity of $W(y^+)$; the results, namely that scaling with characteristic length $\beta^{-(\sigma+1)/2}$ is proper in a patch near where $W = \beta - \epsilon_t^2$, i.e. near where $y^+ = y_m^\beta$, leads to the further question of functional dependence between y_m^β and β . This information, then, would provide the proper scaling at any given point in I . Such information depends on knowledge of some salient features of the function W .

The needed information can be found, in order of magnitude, by the method shown in Fife *et al.* (2005*b*) and Fife *et al.* (2005*a*). That method consists in (1) using the fact that the derivative

$$A(\beta) \equiv - \left. \frac{d^2 \hat{T}}{d\hat{y}^2} \right|_{y^+ = y_m^\beta} = O(1)$$

(since \hat{T} and \hat{y} are the properly scaled variables in that patch—in fact arguments based on the lack of β dependence in (6.12) and the values of the terms at $y^+ = y_m^\beta$ can be given to support the assumption that A is approximately β -independent in certain intervals); and (2) differentiating the identity

$$\left. \frac{d\hat{T}}{d\hat{y}} \right|_{y^+ = y_m^\beta} = 0 \quad (6.17)$$

with respect to β and expressing the result in terms of $A(\beta)$.

For example, one obtains

$$\frac{dy_m^\beta}{d\beta} = -A^{-1} \beta^{-(3+\sigma)/2}. \quad (6.18)$$

Since it can be assumed that $A = O(1)$ and is positive, it is bounded above and below by positive constants independent of β . Applying such bounds to the factor A^{-1} in (6.18) and integrating the resulting inequalities provides the result that the location y_m^β of a scaling patch is asymptotically proportional to the characteristic length $\beta^{-(\sigma+1)/2}$ in that patch. That gives an approximate (asymptotically valid for large y_m^β in this case) relation between β and y_m^β . One then recalls the fact that β is also, by (6.5), related to $dT^+/dy^+ = \beta - \epsilon_t^2$ evaluated at the location of that patch. Integrating this provides an order of magnitude expression as follows for $T^+(y^+)$. The symbol C will denote several different unknown constants which are independent of β and y^+ , and the symbol \approx means equality in order of magnitude only:

$$T^+(y^+) \approx -CA^{-2/(\sigma+1)}(y^+ - C)^{-(1-\sigma)/(1+\sigma)} - \epsilon_t^2 y^+ + C, \quad (6.19)$$

Information on the profile $U^+(y^+)$ can now be found by integrating (6.19):

$$\frac{dU^+}{dy^+} + T^+ + \epsilon_t^2 y^+ = 1.$$

When this is combined with (6.19), the terms in $\epsilon_t^2 y^+$ cancel. With one final integration, the result is:

$$U^+ \approx \begin{cases} CA^{-2/(1+\sigma)}(y^+ - C)^{2\sigma/(\sigma+1)} + C, & \sigma > 0, \\ CA^{-2} \ln(y^+ - C) + C, & \sigma = 0. \end{cases} \quad (6.20)$$

Along the way, one may identify the coefficient m in (6.11) with the derivative of U^+ in (6.20). One verifies that the slope $m = O(\beta^{(1-\sigma)/2})$. This implies that the linear part of the expression for U^+ in (6.9) enjoys the same natural scaling as does the

nonlinear part. The two parts may be combined and that expression written

$$U^+ = U_m^+ + \beta^{-\sigma} \tilde{U}(\hat{y}), \quad (6.21)$$

where the function $\tilde{U} = O(1)$.

This way, calculations based on the $O(1)$ nature of A can be used to obtain qualitative features of the profiles of T^+ and U^+ .

The expressions (6.20) indicate that, asymptotically for large y^+ , the rate of growth of $U^+(y^+)$ depends on σ , and it is logarithmic for $\sigma = 0$. That function decreases when $\sigma < 0$, so that case can be excluded. The case $\sigma = 0$ appears to provide the least positive growth rate for U^+ , resulting in the flattest profile in the core region.

All this was for a given interval I . To maximize the results, one would seek an interval which is as large as possible, and this leads to consideration of the global qualitative nature of the function W . That is the next topic to be examined.

7. Parameter-induced transitions between Couette and Poiseuille flows

Figure 3 depicts the transition from Poiseuille (top) to Couette flow as τ_u^+ passes from -1 to 1 . The objective in this section will be to examine the operative mechanisms for this transition, particularly in view of the scale hierarchies brought out in §6.

7.1. Global properties of W

It turns out that when $\epsilon \ll 1$, the function W takes on one of the three possible shapes described here.

- A. A peak occurs near each of the two walls, with a core region, much larger than the wall regions, in-between (see figure 3*a*, the top two cases). The pure Poiseuille profile is prototypical for this case.
- B. A peak is near the lower (stationary) wall, with a smooth approach to the value 0 as the opposite wall is approached (see the middle case in that same figure).
- C. A peak is near the lower wall and an antipeak (negative minimum or valley) near the upper wall (see the bottom two cases in that same figure). The pure Couette profile is prototypical for this case.

Consider now the evolution of the function W as the parameter τ_u^+ passes continuously from -1 (pure Poiseuille case) to 1 (pure Couette). The changes are seen in graphs of figure 3(*a*), passing from top to bottom. As τ_u^+ increases from the value -1 , the peak near the upper wall becomes smaller. The value of W in the core region, which is negative, increases slightly so as to maintain the required constraint

$$\int_0^2 W(\eta) d\eta = 0. \quad (7.1)$$

Eventually, for some intermediate value $\tau_u^+ = \tau_0$, the upper peak vanishes and type B is reached. After that, a negative peak appears and grows until type C appears with both the positive and the negative peaks having the same amplitude (bottom frame). This is pure Couette flow.

It will now be argued that τ_0 is (at least approximately) 0. If $\tau_0 > 0$, say, and $\tau_0 = O(1)$, then since τ_0 is the ratio of inner length scales in the upper and lower wall regions, the upper inner scale is comparable to the lower one, and when viewed with the lower scaled variable y^+ (as in figure 3), the typical wall structure, including an $O(1)$ peak in the Reynolds stress gradient W , will be evident near

the upper wall. This implies case A. Similarly, if $\tau_u^+ < 0$, $|\tau_u^+| = O(1)$, we are in case C. Therefore, in case B, necessarily $\tau_u^+ = 0$, at least approximately. Since ϵ is the only other parameter in the problem, it specifically follows that $\tau_0 = o(1)$ as $\epsilon \rightarrow 0$.

7.2. Generally there exist two hierarchies

Consider now the hierarchy analysis for type A (peaks near each of the two walls). There will be an interval I , as explained above, on which $dT^+/dy^+ = W$ is a decreasing function, extending from near the peak near the lower wall to the place in the core region where W is minimal. According to the above, each point y^+ in I is the location of a scaling patch with characteristic length $\beta^{-1/2}$, where $\beta - \epsilon_t^2$ is the value of W for that particular y^+ , i.e. $\beta - \epsilon_t^2 = W(y_m^\beta)$.

Symmetry suggests that something similar happens in the corresponding interval I' extending from near the location where W is minimal to the peak near the upper wall. To do this in a systematic way, use the variable $\tilde{y}^+ = 2\epsilon^{-2} - y^+$, measuring distance away from the upper wall, and define $\tilde{T}(\tilde{y}^+) = -T(2\epsilon^{-2} - \tilde{y}^+)$. Then $dT^+/dy^+ = d\tilde{T}/d\tilde{y}^+$. What this means is that in the interval I' , where $W = dT^+/dy^+$ is increasing as a function of y^+ , $\tilde{W} = d\tilde{T}/d\tilde{y}^+$ will be a decreasing function of \tilde{y}^+ . The above analysis can therefore be applied to \tilde{W} on I' .

As a result, adjusted Reynolds stresses

$$\tilde{T}^\beta = \tilde{T} + (\epsilon_t^2 - \beta)\tilde{y}^+ \quad (7.2)$$

can be defined and used as before. Each point in the interval I' is the location of a scaling patch with characteristic length $\beta^{-1/2}$, where β is the value $(dT^\beta/dy^+)(y^+) - \epsilon_t^2$ for that particular point, now in the interval I' leading to the vicinity of the peak near the upper wall.

Two hierarchies are thereby obtained. One leads from the peak near the lower wall, where the characteristic length is least, to the centre region of the channel, where it is maximal. The maximal characteristic length is $O(\epsilon^{-2})$ because that patch accounts for an $O(1)$ fraction of the entire width of the channel, which is $2\epsilon^{-2}$. The other hierarchy comes from the opposite side. In the case of pure Poiseuille flow, the function W is exactly symmetric (even) with respect to the centreline, and the two hierarchies are mirror images of each other with respect to the place where W takes its minimum. But when Type A occurs without exact symmetry, the two hierarchies are only qualitative images of each other, and the location of the minimum of W is not exactly at the centreline.

Consider next type C, when the peak near the upper wall is inverted to become a valley. The change in the reasoning now simply involves redefining $\tilde{T}(\tilde{y}^+) = T^+(2\epsilon^{-2} - \tilde{y}^+)$, and $\tilde{T}^\beta = \tilde{T}^+ + (\epsilon_t^2 - \beta)\tilde{y}$ (formally the same as (7.2)). This gives a second hierarchy with properties similar to the first.

Finally, consider the in-between case of type B. There is only one peak, namely the one near the lower wall, and the interval I extends all the way from there to the upper wall. There is only one hierarchy, with that same domain, and the patch with maximal characteristic length is the one adjacent to the upper wall. It may seem strange that there is no ‘wall layer’ at the upper wall, until one considers that type B occurs only under a very special condition; more or less, that condition says that the differential motion of the wall exactly matches the momentum input of the pressure gradient, and thus effectively removes any pressure-driven stress gradient balance layer near the upper wall.

7.3. Other features of the transition from Poiseuille to Couette

Other characteristic features of the transition from Poiseuille to Couette flow relate to the behaviour of $W = dT^+/dy^+$ with changes in the parameter τ_u^+ . Specifically, for $\tau_u^+ = -1$ the condition (7.1) is separately satisfied on each half of the channel. (Recall that for this case the outer flow approximation to (4.2) is $dT^+/d\eta = -1$.) As τ_u^+ increases from the value -1 , (7.1) is satisfied by a W function that retains its positive peak, as well as a diminished one near $\eta = 2\delta^+$, but has a negative portion that simultaneously decreases in amplitude while covering a greater portion of the channel. For $\tau_u^+ = 0$, W is negative over the entire region $1 < \eta < 2$, and rapidly rises to zero right at $\eta = 2$. By noting that for this case the outer flow approximation to (4.2) is $dT^+/d\eta = -1/2$, one can surmise that, except in a small sublayer near $\eta = 2$, the entire channel is analogous to the region $0 < \eta < 1$ in pure Poiseuille flow. For further increases in τ_u^+ the flow becomes Couette-like and a negative peak in W forms near the upper wall. The function W will then have a single zero, which remains in $0 < \eta < 1$. Coincident with this, (7.1) is satisfied by there being a diminished magnitude of the negative W plateau in the central core and a migration of its zero crossing toward $\eta = 1$. This process culminates (pure Couette flow) with a W function that crosses zero at $\eta = 1$ and that has very small amplitudes except near the upper and low walls respectively.

As discussed above, there generally exist two hierarchies in the channel. Based upon the behaviours of the mean vorticity distribution, however, one may surmise that these hierarchies can be physically distinct, depending on whether the flow is of the Poiseuille or Couette type. In connection with this, it is important to note that Poiseuille-type flows are composed of two adjacent layers of opposing sign mean vorticity, while Couette-type flows comprise one single-signed layer of mean vorticity. Thus, increasing the Couette component (on the Poiseuille side of $\tau_u^+ = 0$) serves to destroy the hierarchy associated with the layer of opposing sign mean vorticity in the region $\eta > 1$. Furthermore, once on the Couette side of $\tau_u^+ = 0$, continuing evolution toward pure Couette flow generates a scale hierarchy in the region $\eta > 1$ that is associated with the negative peak in W , and that is characterized by a mean vorticity field that has the same sign as that in the region $\eta < 1$. Of course, this process culminates when the entire flow is composed of a stress gradient balance layer. That is, the mean dynamics in pure Couette flow are characterized by a balance between the viscous and Reynolds stress gradients everywhere, and thus the ratio of these two terms is -1 . In the region $\eta < 1$, this evolution toward a ratio $S = -1$ everywhere occurs by the outward migration of a mesolayer structure as depicted in figure 1. In the region $\eta > 1$, a similar process occurs, except in this case the -1 condition is approached via a broadening plateau of negative ratio that emerges and spreads outward from near the upper wall with increasing τ_u^+ . (Recall that for $\eta > 1$, $S \approx 0$ under the condition $\tau_u^+ = 0$.) The limiting condition (pure Couette flow) is realized when the inertial layers associated with these two hierarchies is diminished to a zone of zero width at the channel centreline.

Finally, a word of explanation is appropriate regarding the schematic diagram of S (second panel from the bottom, figure 3*b*). Assume the parameter values $\tau_u^+ = 0.2$, $Re_\tau = 150$. Dividing (5.5) by W , one obtains the following expression: $S = -1 - c/W$, where $c = 0.003$. Since $W < -c$ in a small interval near the upper wall, the ratio S is also negative, attaining a negative minimum, in that interval, as shown. This is the beginning of the negative plateau broadening process described above. As τ_u^+ further increases to 1, c decreases to 0 and S attains its uniform state of -1 .

8. Discussion

The method of seeking scaling patches in the context of the unintegrated averaged momentum balance equation was introduced in previous papers by the present authors and P. McMurtry. It is shown here that the analysis of C-P flows also naturally fits within this overarching framework, and thus the present effort provides a detailed picture of how individual Couette and Poiseuille components comprise combined C-P flows. Similarly, since Couette and Poiseuille are subsets of C-P flow, the results in this paper automatically encompass the mean flow (U^+ and T^+) scaling behaviours of the two pure flows individually. In fact some perspectives and results in the present paper are new, even when confined to the context of the pure flows.

These C-P flows can be formulated in terms of two parameters: a large Reynolds number Re_τ and a parameter τ_u^+ designating the ratio of shear stresses at the upper and lower walls. As this ratio passes from -1 to 1 , the character of the flow changes from pure Poiseuille to pure Couette. During this transition, the principal layer structure of the flow, as revealed for the Poiseuille case in Wei *et al.* (2005a), changes also: at various points, the number of layers (not scaling patches) is reduced from four to three and then to one, finally reaching the Couette state in which there is only a single layer, the stress gradient balance layer.

Further details about the flow profiles at these transition points, as well as the critical values of the parameters, require additional study. In particular, such an effort would benefit from high quality data sets spanning a greater range of parameters.

Continua (hierarchies) of length scales described in terms of scaling patches were shown in previous work to be core phenomena in turbulent channel flows, and that continues to be the case in the C-P flow scenarios. The scaling structure, including the distribution of patches, is most clearly described in reference to the properties of the function $W(y^+) \equiv (dT^+/dy^+)(y^+)$. Qualitative changes in the function W induced by changes in τ_u^+ reveal, for example, the mechanism operative in the transition between pure Poiseuille and Couette flows.

Appendix. The inner-scaling patch at the wall

The construction of the mesoscaling patch given in § 5.1 has, as a primary ingredient, the fact that as the peak in Reynolds stress is approached, a region must appear in which all three terms in the mean momentum balance equation, (5.5), will have the same order of magnitude. This is simply because the gradient (dT^+/dy^+) approaches 0. There will, of course, be a smaller region encompassing the peak in which the last term on the left of (5.5) has smaller order of magnitude than the others, because it vanishes at the peak.

A similar phenomenon happens when $y^+ \rightarrow 0$, since that same gradient is zero at the wall ($y^+ = 0$) and positive for small values of $y^+ > 0$. The same conclusion may therefore be deduced: in a small region near the wall, all three terms in (5.5) will have the same order of magnitude. But the argument in § 5.1 can only partially be continued beyond this stage to produce a patch with different scaling; in fact it is well known (see also the reason given below) that the characteristic length scale arbitrarily near the wall remains the inner scale. The reason the argument is no longer completely valid will now be explained. In addition, the correctly scaled mean momentum balance very near the wall will be derived.

There have been many analytical, empirical, and computational studies of the properties of the near-wall region; we mention only Cenedese, Romano & Antonia (1998), as our results fit particularly well with theirs. Our purpose here is to show

that a scaling patch exists there, whose derivation and description fits within the framework of the methodology developed here and in our previous papers.

At the wall, additional constraints are imposed on the functions U^+ and T^+ , besides the basic differential equation (5.5). First of all, the very definition of inner scaling requires an automatic boundary condition $dU^+/dy^+(0) = 1$. The inner scaling was chosen just so that condition holds. Secondly, the no-slip condition requires the boundary conditions

$$U^+(0) = T^+(0) = \frac{dT^+}{dy^+}(0) = \frac{d^2T^+}{dy^{+2}}(0) = 0.$$

The first requirement is simply a result of our choice of normalized variables y^+ and U^+ , and is not a statement of any physical constraint. The other boundary conditions result from a physical effect located at the wall. They have no analogue at the mesoscaling patch, and constitute the basic reason that the present construction is different from the mesoscale construction.

If one proceeds in the same vein as before on the basis of (5.1) and (5.2), the effect of the first boundary condition $(dU^+/dy^+)(0) = 1$ is that the length scale in that patch is given by $\alpha = 1$. This means that $\hat{y} = y^+$: the length scale in that patch is the same as that with the original inner-normalized scaling. This is of course almost a tautology.

But then the rest of the argument, following (5.5), in which α and γ are determined, can no longer be carried out as it stands, since α has already been determined. However, one can proceed after some reformulation of the problem.

At this point, the first substantial difference in method emerges between the derivation of the mesoscale patch and the present argument for what we shall call the wall patch. As mentioned, it is allied with the physical no-slip constraint. In both cases, we look for scaled solutions of (5.5) in a neighbourhood of a maximum or minimum of T^+ . The first term, ϵ_t^2 , in that equation is a forcing term, which derives from the imposed pressure gradient.

In both the mesoscale case and the present wall case, a scaling, namely a choice of α , γ , λ in (5.1), (5.2), is sought which will render the three terms of (5.5) the same formal order of magnitude. A unique choice is only possible if one of these three factors is specified by other means. In the mesoscale case, empirical data having to do with the velocity increment across the patch, and also the rate of growth of U^+ in the hierarchy, is used to select the value $\lambda = 1$, while leaving open the additional possibility of other choices leading to different growth rates. This serves to determine the other two factors. In the wall patch, where this argument is not applicable, the definition of the inner scaling requires $\alpha = 1$, and the equality criterion now can be used to determine γ and λ . Namely, evaluating the three terms of (2.2) under the transformation (5.1), (5.2) with $\alpha = 1$ tells us that $\gamma = \lambda = \epsilon_t^2$. In neither case does this provide the value of m , because the derivatives in (5.5) annihilate the linear term. However, the value of m was obtained by other means: through use of (6.19) and the connection T has with the slope, in the case of patches embedded in the hierarchy, and by means of the boundary condition giving the slope at the wall, in the present case.

The scaled version of (5.5) in that patch is

$$1 + \frac{d^2\hat{U}}{dy^{+2}} + \frac{d\hat{T}}{dy^+} = 0. \quad (\text{A } 1)$$

The individual terms of this equation are known only at $y^+ = 0$; but it provides a linear relation between the two derivatives. This equation is the analogue of (5.11), and is in the form of a balance of three rescaled forces.

In short, there is a scaling patch near the wall, no doubt including the traditional viscous sublayer, in which the inner length scale is correct, but the deviations of the functions U^+ and T^+ from their linear parts depend on Re_τ like $\epsilon_\tau^2 \approx (Re_\tau)^{-1}$.

Finally, as y^+ enters the patch from above, there is a balance exchange from layer II, where the viscous and turbulent forces balance, to layer I, where the pressure gradient balances the viscous plus turbulence force.

The location of this exchange, and in fact the size of layer I, is $O(1)$ in wall units, because that is the length scale for the parameterless (A 1).

In terms of the traditional buffer and logarithmic layer, we surmise that they lie outside layer I, which can be identified as the viscous sublayer (although at its outer edge the viscous and turbulent forces are equal in order of magnitude). Outside that layer is approximately where the hierarchy begins (say $y^+ \approx 7$), which is also where the traditionally defined buffer layer begins. The logarithmic mean profile approximation associated with the hierarchy, however, does not become valid until distances from the beginning of the hierarchy are sufficient for A in (6.18) to be approximately constant.

The dependence of U^+ and T^+ in layer I on the parameter τ_u^+ is seen in the scaling there of the nonlinear parts. The factor is ϵ_τ^2 , which is defined (5.7) in terms of that parameter.

REFERENCES

- AFZAL, N. 1982 Fully developed turbulent flow in a pipe: An intermediate layer. *Ingenieur-Archiv* **52**, 355–377.
- ANTONIA, R. A., TEITEL, M., KIM, J. & BROWNE, L. W. B. 1992 Low Reynolds number effects in a fully developed turbulent channel flow. *J. Fluid Mech.* **236**, 579–605.
- CENEDESE, A., ROMANO, G. P. & ANTONIA, R. A. 1998 A comment on the linear law of the wall for fully developed turbulent channel flow. *Exps. Fluids* **25**, 165–170.
- EL TELBANY, M. M. M. & REYNOLDS, A. J. 1980 Velocity distributions in plane turbulent channel flows. *J. Fluid Mech.* **100**, 1–29.
- EL TELBANY, M. M. M. & REYNOLDS, A. J. 1981 Turbulence in plane channel flows. *J. Fluid Mech.* **111**, 283–318.
- FIFE, P., KLEWICKI, J., MCMURTRY, P. & WEI, T. 2005a Multiscaling in the presence of indeterminacy: Wall-induced turbulence. *Multiscale Model. Simul.* **4**, 936–959.
- FIFE, P., WEI, T., KLEWICKI, J. & MCMURTRY, P. 2005b Stress gradient balance layers and scale hierarchies in wall-bounded turbulent flows. *J. Fluid Mech.* **532**, 165–189.
- IWAMOTO, K., SUZUKI, Y. & KASAGI, N. 2002 Reynolds number effect on wall turbulence: Toward effective feedback control. *Intl J. Heat Fluid Flow* **23**, 678–689.
- IZAKSON, A. 1937 On the formula for the velocity distribution near walls. *Tech. Phys. USSR* **IV**, **2**, 155–162.
- KLEWICKI, J., MCMURTRY, P., FIFE, P. & WEI, T. 2004 A physical model of the turbulent boundary layer consonant with the structure of the mean momentum balance. In *15th Australasian Fluid Mech. Conf.* The University of Sydney, Sydney, Australia.
- KURODA, A., KASAGI, N. & HIRATA, M. 1994 Direct numerical simulation of turbulent plane Couette–Poiseuille flows: Effect of mean shear on the near-wall turbulence structures. In *Turbulent Shear Flows 9* (ed. F. Durst et al.). Springer.
- LIBBY, P. A. 1996 *Introduction to Turbulence*, 1st edn. Taylor and Francis.
- MILLIKAN, C. B. 1939 A critical discussion of turbulent flows in channel and circular tubes. In *Proc. 5th Int. Congr. Applied Mechanics* (ed. J. P. Den Hartog & H. Peters). Wiley.
- MOSER, R. D., KIM, J. & MANSOUR, N. N. 1999 Direct numerical simulation of turbulent channel flow up to $Re_\tau = 590$. *Phys. Fluids* **11**, 943–945.

- NAKABAYASHI, K., KITO, O. & KATO, Y. 2004 Similarity laws of velocity profiles and turbulence characteristics of Couette–Poiseuille turbulent flows. *J. Fluid Mech.* **507**, 43–69.
- PANTON, R. L. 1984 *Incompressible Flow*, 1st edn. Wiley.
- PANTON, R. L. 1997 A Reynolds stress function for wall layers. *Trans. ASME: J. Fluids Engng* **119**, 325–330.
- SCHLICHTING, H. & GERSTEN, K. 2000 *Boundary Layer Theory*, 8th edn. Springer.
- SHINGAI, K., KAWAMURA, H. & MATSUO, Y. 2000 DNS of turbulent Couette flow and its comparison with turbulent Poiseuille flow. In *Advances in Turbulence 8: Proc. 8th European Turbulence Conference*, p. 972. Aichi Shuppan, Japan.
- SREENIVASAN, K. R. 1989 The turbulent boundary layer. In *Frontiers in Experimental Fluid Mechanics* (ed. Gad el Hak), pp. 159–209. Springer.
- TENNEKES, H. & LUMLEY, J. L. 1972 *A First Course in Turbulence*. MIT Press.
- THURLOW, E. M. & KLEWICKI, J. 2000 Experimental study of turbulent Poiseuille–Couette flow. *Phys. Fluids* **12**, 865–875.
- WEI, T., FIFE, P., KLEWICKI, J. & MCMURTRY, P. 2005a Properties of the mean momentum balance in turbulent boundary layer, pipe and channel flows. *J. Fluid Mech.* **522**, 303–327.
- WEI, T., MCMURTRY, P., KLEWICKI, J. & FIFE, P. 2005b Mesoscaling of Reynolds shear stress in turbulent channel and pipe flows. *AIAA J.* **43**, 2350–2353.